Protein Science (1997), *6*:1858–1868. Cambridge University Press. Printed in the USA.

Conformational studies of the N-terminal lipid-associating domain of human apolipoprotein C-I by CD and ^{1}H NMR spectroscopy

ANNETT ROZEK,[1] GARRY W. BUCHKO,[1,3] PATRICK KANDA,[2,4] AND ROBERT J. CUSHLEY[1]

[1]Department of Chemistry and Institute of Molecular Biology and Biochemistry, Simon Fraser University, Burnaby, British Columbia, V5A 1S6, Canada
[2]Department of Virology and Immunology, Southwest Foundation for Biomedical Research, San Antonio, Texas, 78228-0147

(RECEIVED February 24, 1997; ACCEPTED May 7, 1997)

Abstract

A peptide comprising the N-terminal 38 residues of human apolipoprotein C-I (apoC-I(1–38)) was synthesized using solid-phase methods and its solution conformation studied by CD and ^{1}H NMR spectroscopy. The CD data indicate that apoC-I(1–38) has a similar helical content (55%) in the presence of saturating amounts of SDS or egg yolk lysophosphatidylcholine. A structural ensemble of SDS-bound apoC-I(1–38) was calculated from 464 NOE-based distance restraints using distance geometry methods. ApoC-I(1–38) adopts a helical structure between residues V4 and K30 and an extended C-terminus from Q31 when associated with SDS. The region K12–G15 undergoes slow conformational exchange as indicated by above-average amide resonance linewidths, large temperature coefficients, and fast exchange (<2 h) of backbone amide protons with deuterium. The mobility of K12–G15 is reflected in the poorly defined dihedral angles of K12 and E13 in the calculated ensemble of structures. The average structure of apoC-I(1–38) is curved toward its hydrophobic face with bends of 125°, centered at K12/E13, and 150°, centered at K21. This curvature appears to be driven by the interaction of two hydrophobic clusters, one formed by residues L8, L11, F14, and L18, and the other by L25, I26, and I29, with the amphiphile SDS. Based on our present structural definition of apoC-I(1–38) and the previously obtained structure of the fragment apoC-I(35–53), we propose the secondary structure of intact apolipoprotein C-I.

Keywords: curved amphipathic helix; LCAT activation; lipid association; peptide synthesis; SDS; slow chemical exchange

Human apolipoprotein (apo) C-I is a 57-residue exchangeable apolipoprotein distributed mainly in HDL and VLDL. HDL facilitates the uptake of cholesterol from peripheral tissue, and low plasma concentrations of HDL have been associated with the development of coronary heart disease (Miller & Miller, 1975). The enzyme lecithin:cholesterol acyltransferase (LCAT) catalyzes the conversion of free cholesterol to cholesteryl ester, a reaction that occurs preferentially on HDL particles (Glomset, 1968). LCAT is primarily activated by apoA-I, whereas apoC-I serves as a secondary activator (Soutar et al., 1975; Jonas, 1986). For instance, apoC-I stimulates LCAT activity up to 78% as effectively as apoA-I in POPC proteoliposomes containing cholesterol (Steyrer & Kostner, 1988). ApoC-I may become important for patients suffering from dyslipoproteinemias, such as Tangier disease and familial apoA-I and apoC-III deficiency (Clifton-Bligh et al., 1972; Schaefer et al., 1985). In both conditions, the plasma of patients displays a normal free cholesterol/cholesteryl ester ratio despite having a dramatically lowered apoA-I concentration, and therefore, apoC-I may be the active cofactor. ApoC-I inhibits the uptake and degradation of triglyceride-rich lipoproteins from human plasma by the apoE-dependent LDL receptor (Sehayek & Eisenberg, 1991) and was reported to inhibit the binding of β-VLDL to the LDL receptor-related protein, probably by displacing apoE from the VLDL surface (Weisgraber et al., 1990; Swaney & Weisgraber, 1994).

Reprint requests to: R.J. Cushley, Institute of Molecular Biology and Biochemistry; Simon Fraser University; Burnaby, British Columbia, Canada; V5A 1S6; e-mail: cushley@sfu.ca.

[3]Present address: Battelle Pacific Northwest National Laboratory, Macromolecular Structure and Dynamics, P.O. Box 999, Richland, Washington 99352.

[4]Present address: BioSynthesis Inc., 612 E. Main Street, Lewisville, TX 75057.

Abbreviations: HDL, high density lipoprotein; VLDL, very low density lipoprotein; POPC, L-α-1-palmitoyl-2-oleoylphosphatidylcholine; LDL, low density lipoprotein; SDS, sodium dodecyl sulfate; NOESY, nuclear Overhauser enhancement spectroscopy; TOCSY, total correlated spectroscopy; DQF-COSY, double quantum filtered correlated spectroscopy; LCAT, lecithin:cholesterol acyltransferase; AMPDA, aminomethyl polydimethylacrylamide; CETP, cholesteryl ester transfer protein; CSI, chemical shift index; DSS, 4,4-dimethyl-4-silapentane-1-sulfonate; DSSP, description of secondary structure in proteins; TFE, trifluoroethanol.

ApoC-I(1–38) is the larger of the two fragments generated by cyanogen bromide cleavage of apoC-I and has affinity for lipid (Jackson et al., 1974). In some baboon families, the analogous region, corresponding to the N-terminal 38 residues of baboon apoC-I, was shown to exist as a unique protein in plasma and to exert an inhibitory effect on CETP (Kushwaha et al., 1993). Human apoC-I(1–38) inhibits baboon CETP 64% as effectively as the baboon apoC-I(1–38) (Kanda et al., 1994). The enzyme CETP is responsible for the transfer of cholesteryl ester from HDL to VLDL and LDL (Morton & Zilversmit, 1982; Tall, 1993) and, in some individuals, decreased CETP activity leads to high HDL levels (Koizumi et al., 1985, 1991; Yokoyama et al., 1986). CETP inhibitor proteins in human plasma, M_r = 29,000–32,000, have been reported (Son & Zilversmit, 1984; Nishide et al., 1989; Morton & Steinbrunner, 1993; Morton & Greene, 1994), however, a distinct human apoC-I(1–38) has never been identified.

The structure–function relationships of apolipoproteins are not well understood due to a paucity of information regarding their conformation and mode of lipid association. The main structural motif predicted to facilitate the interaction of the exchangeable apolipoproteins with lipids is the amphipathic helix, which is defined as an α-helix with opposing polar and nonpolar faces (Segrest et al., 1974, 1992). ApoC-I is postulated to form two class A_2 helices, residues 7–32 and 33–53, with the positively charged amino acid residues clustering at the polar–nonpolar interface and the negatively charged amino acid residues at the center of the hydrophilic face (Segrest et al., 1990, 1992).

Previous structural studies of 18 to 24-residue long fragments of apoC-I (Rozek et al., 1995), apoA-I (Wang et al., 1996b), apoA-II (Buchko et al., 1996), and apoE (Wang et al., 1996a) in the presence of SDS or DPC have confirmed the formation of an amphipathic helix. In this report, we extend the study to a longer apolipoprotein fragment, apoC-I(1–38), corresponding to two-thirds of apoC-I and containing the predicted N-terminal lipid-binding region. CD experiments with apoC-I(1–38) were performed in the presence of SDS and egg yolk lysoPC to assess possible structural differences of the peptide depending on the amphiphilic head group of the detergent. The conformation of apoC-I(1–38), calculated from NMR data in the presence of SDS, is compared to the conformation of the previously studied peptide apoC-I(7–24)

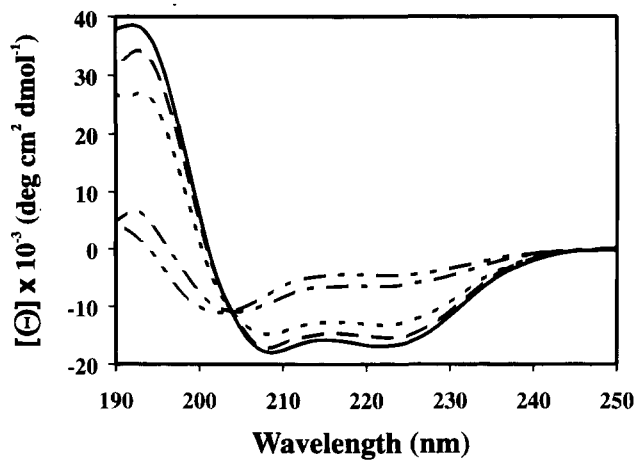

Fig. 1. CD spectra of apoC-I(1–38) at 25 °C and various molar ratios of peptide:SDS: 1:0 (— - - — - -), 1:1 (— - — - — -), 1:5 (- - - - - - - - - -), 1:10 (— — — —), and 1:20 (———).

(Rozek et al., 1995). Our findings, combined with structural results obtained for apoC-I(35–53) (Rozek et al., 1995) and related to activity studies on various apoC-I fragments with LCAT (Sparrow et al., 1977), lead us to propose the structure of intact apoC-I and a model for its mode of lipid association.

Results

CD spectroscopy

The CD spectra from the titration of an aqueous solution of apoC-I(1–38) with SDS are presented in Figure 1. In the absence of SDS, the CD spectrum shows a strong negative band near 200 nm, characteristic of a peptide without a well-defined secondary structure (Woody, 1977). Upon the stepwise addition of SDS, the spectra increasingly assume the double minimum at 208 and 222 nm, and the maximum at 195 nm, indicative of a helical conformation (Holzwarth & Doty, 1965). Above a molar SDS to peptide ratio of 20, no further changes were observed, indicating a saturation of the

Table 1. *Helical content (%) of ApoC-I(1–38) obtained from the titration with SDS and egg yolk LysoPC (EYLL)*[a]

Molar ratio of detergent:peptide	% Helix (SDS)[b]	% Helix (EYLL)[b]	$[\Theta]_{222}$ (SDS)[c]	% Helix (SDS)[d]	$[\Theta]_{222}$ (EYLL)[c]	% Helix (EYLL)[d]
0	13	13	−3,970	20	−3,970	20
1	18	19	−6,260	24	−5,310	21
5	42	36	−12,710	40	−9,470	32
10	47	42	−15,410	47	−12,460	40
20	57	56	−16,090	49	−15,610	48
40	54	60	−17,410	52	−16,410	50
60	54	58	−17,910	54	−16,600	50
80	54	50	−18,800	56	−16,940	52

[a]CD data were collected in aqueous solution at 25 °C and pH 6.
[b]Helical content was estimated by deconvoluting the CD spectra using convex constraint analysis (Perczel et al., 1992).
[c]$[\Theta]_{222}$ values are in units of deg × cm^2/dmol.
[d]Helical content was estimated using the relation: % Helix = ($|[\Theta]_{222}|$ + 3,000)/(36,000 + 3,000) (Greenfield & Fasman, 1969).

peptide with the detergent. To investigate the influence of the amphiphilic head group on the helical content of apoC-I(1–38), the titration results obtained with SDS, which contains an anionic head group, were compared to those obtained with egg yolk lysoPC, which contains a zwitterionic lipid head group. The helical content of apoC-I(1–38), adopted in either SDS or egg yolk lysoPC solution, was estimated by convex constraint analysis of the CD spectra (Perczel et al., 1992) and from the $[\Theta]_{222}$ value (Greenfield & Fasman, 1969) (Table 1). A comparison between SDS and egg yolk lysoPC reveals no major differences; saturation of the peptide with the detergent is established at a molar ratio of detergent to apoC-I(1–38) of 20. The helical content of apoC-I(1–38) bound to saturating amounts of SDS and egg yolk lysoPC, estimated by averaging the values obtained by convex constraint analysis over the detergent to peptide ratios 20–80, is identical at 55%.

The influence of temperature and pH on the helical content of apoC-I(1–38), saturated with the amphiphile, was also investigated. In both SDS and egg yolk lysoPC solutions, less than 3% change in helicity was observed by varying the temperature between 10 °C and 37 °C. With egg yolk lysoPC, the helical content of apoC-I(1–38) varied by 3% in the pH range 3–9. In SDS solution, the helical content varied by 3% in the pH range 3–6, whereas a 10% decrease was noted between pH 6 and 9. The drop in helical content of apoC-I(1–38) in SDS solution in the basic pH range may be due to electrostatic repulsion between the deprotonated carboxyl group of residue E19, which was shown to reside at the polar–nonpolar interface of the amphipathic helix calculated for apoC-I(1–38), and the SDS head groups. In egg yolk lysoPC, the negatively charged E19 carboxyl group may be counterbalanced by the positive charge in the phosphocholine head group, leading to similar helicity in the acidic and basic pH range.

Proton resonance assignments

The NMR experiments were performed at a molar SDS to apoC-I(1–38) ratio of 60 and an SDS concentration of 300 mM, well above the critical micelle concentration, to ensure the formation of uniform peptide–SDS complexes (McDonnell & Opella, 1993). The TOCSY spectrum showed a poor magnetization transfer between most backbone amide and side-chain protons (Fig. 2). The effect is likely due to small $^3J_{HN\text{-}H\alpha}$ coupling constants characteristic for α-helices and the large molecular weight of the peptide–SDS complex, which leads to broad amide proton resonances (Henry & Sykes, 1994). However, complete magnetization transfer between backbone amide and side-chain protons was observed for residues D3–A7 and S32–M38, i.e., at both peptide termini, which were shown to be flexible in the structure calculated for apoC-I(1–38). The proton resonances, assigned using the procedures described by Wüthrich (1986) and Englander and Wand (1987), are summarized in Table 2. Where spectral resolution permitted, amino acid spin systems were identified in the H^N-H^α and $H^{\alpha,\beta}$-$H^{side\text{-}chain}$ regions of the TOCSY spectrum and connected via sequential H^N-H^N and H^α-H^N cross-peaks observed in the NOESY spectrum. In cases of resonance overlap, sequential assignments were obtained first by H^N-H^N, H^α-H^N, and H^β-H^N NOE connectivities. Then, tentative side-chain assignments were made from the H^N-$H^{side\text{-}chain}$ region of the NOESY spectrum and adjacent amino acids were matched with the primary sequence. The complete assignment of side-chain resonances was obtained by the detailed analysis of the TOCSY and DQF-COSY spectra. For K10, K21, L11, L25, and R28, the assignment of side-chain protons relied almost exclusively on the NOESY spectrum because their H^α resonances overlapped in the H^α-H^β region of the TOCSY spectrum. In the amide region of the NOESY spectrum, presented in Figure 3, sequential connectivities were established from residue S6 to E13 and F14 to M38. The residues S5 and S6 were distinguished by NOE cross-peaks to D9, which were assigned to S6 $H^{\alpha,\beta}$-D9 H^β and S6 H^α-D9 H^N, consistent with the helical structure indicated by H^α_i-$H^N_{i+3,4}$ cross-peaks of V4 to A7 and L8.

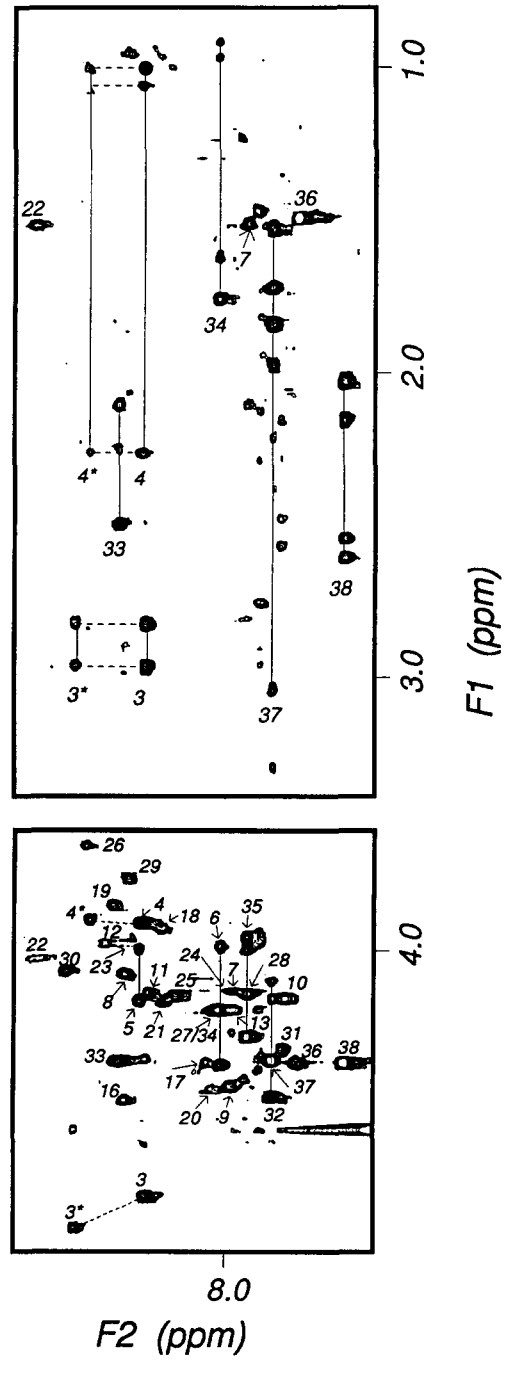

Fig. 2. Fingerprint region of the TOCSY spectrum of apoC-I(1–38) at 37 °C using a spinlock time of 100 ms. H^N-H^α cross-peaks and side-chain cross-peaks of the flexible C-terminus and N-terminus are labeled. The doubled cross-peaks of D3 and V4 are connected by dashed lines.

Table 2. *^1H chemical shifts[a] of human ApoC-I(1–38) in SDS solution at 37 °C and pH 4.8[b]*

Residue	$\Delta\delta/\Delta T$[c]	H^N	H^α	H^β	H^γ	Other	CSI[d]
T1			4.25	4.17	1.46		−1
P2			4.60	2.39, 1.81	2.06, 1.96	H^δ3.91, 3.60	+1
D3	−6.2	8.27	4.80	2.98, 2.82			+1
		(8.50)	(4.91)				
V4	−6.7	8.28	3.90	2.27	1.06, 1.00		−1
		(8.45)	(3.89)				
S5	−5.3	8.28	4.16	3.99			−1
S6	−5.5	8.01	4.36	3.98			−1
A7	−5.2	7.92	4.15	1.51			−1
L8	−8.5	8.34	4.07	1.86, 1.70	1.84	H^δ1.00, 0.94	−1
D9	−5.5	7.98	4.44	2.99, 2.82			−1
K10	−4.8	7.80	4.15	2.06,1.92[e]	1.58[e]	H^δ1.71?, H^ϵ3.02	−1
L11	−7.5	8.26	4.14	1.93	1.87	H^δ0.97, 0.93	−1
K12	−9.7	8.40	3.98	2.00[e]	1.44[e]	H^δ1.80, H^ϵ3.00	−1
E13	−5.2	7.98	4.19	2.24	2.60, 2.48		−1
F14	−7.0	8.43	4.56	3.37, 3.26		2,6H 7.27, 3,4,5H 7.20	0
G15	−9.2	8.90	3.79, 3.61				−1
		(8.79)					
N16	−4.8	8.33	4.49	2.99, 2.90		NH_2 7.44, 6.84	−1
T17	−7.6	8.09	4.06	4.40	1.30		−1
L18	−5.5	8.21	3.91	1.70	1.53	H^δ0.79	−1
E19	−5.5	8.37	3.84	2.32,2.22	2.62		−1
D20	−5.3	8.04	4.45	3.03,2.84			−1
K21	−4.7	8.20	4.16	2.02[e]	1.63[e]	H^δ1.86, H^ϵ2.98	−1
A22	−4.5	8.63	4.02	1.52			−1
R23	−7.3	8.30	3.95	1.97	1.70	H^δ3.29, 3.27, H^ϵ7.18	−1
E24	−5.0	8.00	4.12	2.30, 2.23	2.58, 2.50		−1
L25	−4.8	8.16	4.14	1.92, 1.82	1.73	H^δ0.99, 0.95	−1
I26	−5.2	8.45	3.64	2.01	1.81, 1.22, 0.99	H^δ0.89	−1
S27	−4.4	8.015	4.19	4.05			−1
R28	−5.5	7.92	4.13	2.09	1.88, 1.70	H^δ3.26, 3.19, H^ϵ7.20	−1
I29	−7.5	8.33	3.75	2.07	1.86, 1.16, 0.93	H^δ0.87	−1
K30	−8.7	8.53	4.06	1.98[e]	1.47[e]	H^δ1.71, H^ϵ2.98	−1
Q31	−3.7	7.81	4.32	2.28, 2.15	2.58, 2.47	NH_2 7.35, 6.76	0
S32	−2.9	7.83	4.48	4.10, 4.16			0
E33	−6.9	8.35	4.36	2.24, 2.10	2.49		0
L34	−6.5	8.02	4.19	1.77, 1.62	1.77	H^δ0.96, 0.91	−1
S35	−6.0	7.93	4.27	3.97			−1
A36	−3.3	7.75	4.37	1.49			0
K37	−4.0	7.84	4.36	1.98, 1.84[e]	1.53[e]	H^δ1.71, H^ϵ3.03	0
M38	−2.7	7.59	4.37	2.15, 2.02	2.60, 2.53	H^ϵ2.08	−1

[a]All chemical shifts are referenced to DSS. No stereospecific assignments were made.
[b]Molar ratio of SDS to peptide: 60.
[c]Backbone amide proton temperature coefficients were determined in the temperature range of 25–50 °C at pH 4.8.
[d]The CSI was calculated as described by Wishart et al. (1992) using the random coil H^α chemical shifts determined by Wishart et al. (1995).
[e]Due to low resolution in the DQF-COSY spectrum, the β-protons and γ-protons of lysines were assigned tentatively on the basis of their expected chemical shifts.

Sites affected by chemical exchange

The NMR spectra of apoC-I(1–38) showed doubled cross-peaks that persisted upon increasing the SDS concentration from 300 mM to 480 mM. Two of the additional spin systems, designated D3* and V4*, were assigned to D3 and V4 (Figs. 2, 3). An exchange cross-peak between the amide resonances was observed for V4* and V4, but not for D3* and D3 (Fig. 3), and a strong NOE cross-peak was observed between D3* H^α and V4* H^N. Such observations suggest the presence of two conformations near the N-terminus of apoC-I(1–38) that are in slow exchange on the NMR time scale. A *cis/trans* isomerization of P2 may give rise to such conformational variability; however, P2 was found to assume predominantly the *trans* conformation because strong NOEs were observed between δ-protons of P2 and both α- and β-protons of T1. Alternatively, the presence of two conformations for D3 and V4 may indicate an equilibrium between an SDS bound and unbound N-terminus of apoC-I(1–38).

Two sets of resonances were also observed for G15. An exchange cross-peak between the broadened amide resonances of

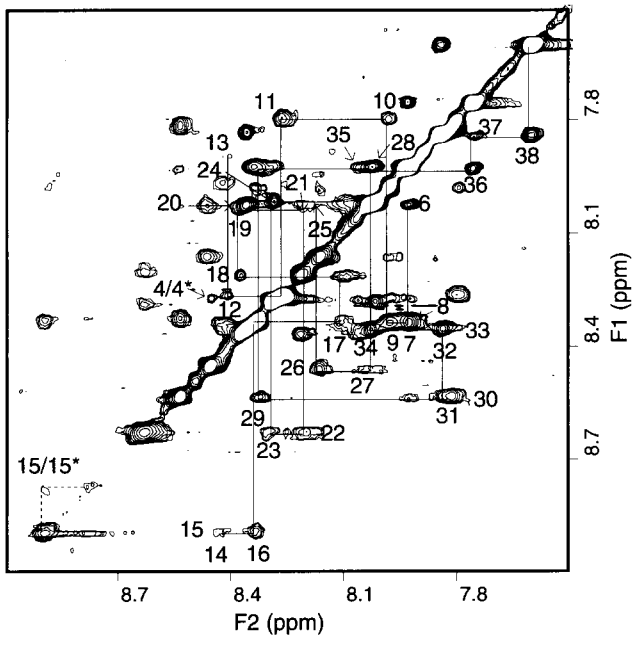

Fig. 3. Amide region of the NOESY spectrum of apoC-I(1–38) at 37° with a mixing time of 200 ms. The sequential assignments and exchange cross-peaks of V4 and G15 are labeled.

G15 and G15* (Fig. 3) suggests the presence of two slowly exchanging local backbone conformations. Support for such an equilibrium is provided by the above-average amide resonance linewidths of K12, E13, and F14, and the large temperature coefficients of the K12 and G15 amide resonances (Table 2). Furthermore, the integral of the upfield G15 amide resonance increases with temperature (25 °C to 50 °C), indicating a shift of the equilibrium toward the conformation represented by the upfield resonance. The calculated structure of apoC-I(1–38) reflects the NOE contacts observed for the conformation represented by the downfield G15 amide resonance, which is dominant at 37 °C (Fig. 3). The NMR spectra of apoC-I(1–38) in SDS solution were compared to the spectra of the peptide in aqueous solution containing 50% TFE, a solvent that promotes helical structure (53%) in apoC-I(1–38) as indicated by CD data. The NMR spectra of apoC-I(1–38) in 50% TFE show only one set of peaks for G15 and the amide resonance linewidths of K12–G15 are similar to the other backbone amide resonances, suggesting that the slow exchange in this region of apoC-I(1–38) is due to interactions between the peptide and SDS.

NOE connectivities and secondary shifts

The sequential and medium-range NOE connectivities observed between backbone protons of apoC-I(1–38) are summarized in Figure 4. The sequential H^N_i-H^N_{i+1} contacts are medium to strong,

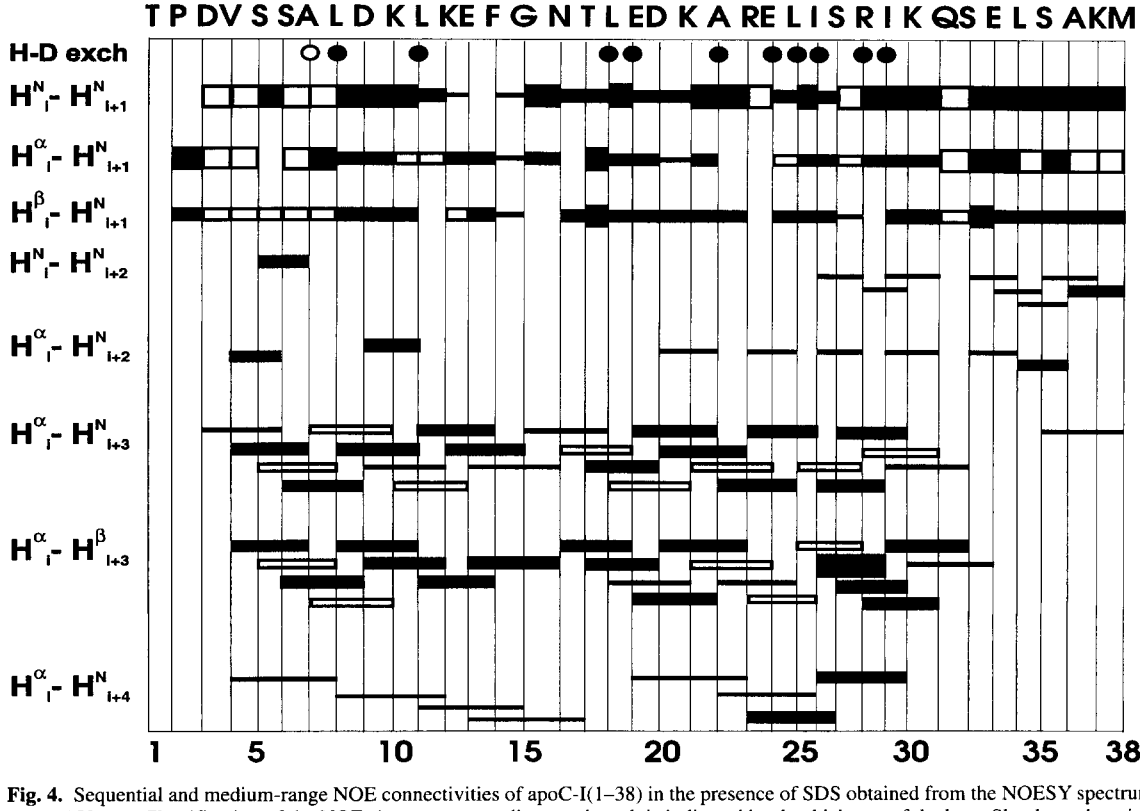

Fig. 4. Sequential and medium-range NOE connectivities of apoC-I(1–38) in the presence of SDS obtained from the NOESY spectrum (τ_m = 150 ms). Classification of the NOEs into strong, medium, and weak is indicated by the thickness of the bars. Slowly exchanging backbone amide protons are represented by filled circles. Open bars and circles refer to ambiguous assignments due to resonance overlap.

whereas most H_i^{α}-H_{i+1}^{N} connectivities are of medium intensity. A helical conformation between residues V4 and K30 is indicated by an abundance of medium-range H_i^{α}-H_{i+3}^{N}, H_i^{α}-H_{i+3}^{β}, H_i^{α}-H_{i+4}^{N} cross-peaks. The CSI of apoC-I(1–38) (Table 2), determined using the method by Wishart et al. (1992), and the random coil H^{α} chemical shifts reported by Wishart et al. (1995), also supports the formation of a helix between V4 and K30. The CSI of F14 is zero, indicating conformational exchange of this residue (Wishart et al., 1991), which is consistent with the absence of the H_i^{N}-H_{i+1}^{N} cross-peak between E13 and F14 and very weak H_i^{N}-H_{i+1}^{N} cross-peaks between K12 and E13, and F14 and G15 (Figs. 3, 4). In addition, weak H_i^{α}-H_{i+3}^{N} contacts exist between D9 and K12, E13 and N16, and G15 and L18 (Fig. 4). In the calculated structure of apoC-I(1–38), these weak restraints lead to a poorly defined helical turn between K12 and G15. The C-terminus of apoC-I(1–38), residues Q31–M38, does not exhibit NOEs characteristic of a well-ordered structure, a feature that is also reflected by the CSI.

Deuterium exchange experiments

The exchange rate of amide protons provides information about the formation of hydrogen bonds (Wagner & Wüthrich, 1982), helix stability (Rohl & Baldwin, 1994), and solvent accessibility (Bai et al., 1993). Amide protons of residues buried in a hydrophobic environment, like the interior of a peptide–SDS complex, are less likely to contact solvent molecules and have longer exchange times than surface amide protons (Spyracopoulos & O'Neil, 1994). In the helical region of apoC-I(1–38), slow exchange (>2 h) was observed primarily for amide protons of hydrophobic residues (Fig. 4). This effect is consistent with an interfacial arrangement of the helix in the peptide–SDS complex with the hydrophobic residues inserted into the micellar interior. Of the hydrophobic residues in the helical region, only F14 has a fast exchanging amide proton, indicating that it is accessible to solvent and does not participate in a hydrogen bond. Such an observation suggests a destabilization of the helical conformation, in agreement with the weak NOE contacts encountered in the region K12–G15.

Calculated structure of ApoC-I(1–38)

The number and distribution of NOE distance restraints used for structure calculation of apoC-I(1–38) is illustrated in Figure 6A. A total of 464 distance restraints (270 interresidue and 194 intraresidue restraints) was used to generate a final set of 30 structures. Of these, 28 structures were selected as representative samples of the conformation of apoC-I(1–38) on the basis of small NOE distance restraint violations. The average number of NOE distance restraint violations >0.1 Å is 2.75 per structure, whereas distance restraint violations >0.01 Å amount to 32.5 per structure. The superposition of 28 backbone structures of apoC-I(1–38) is shown in Figure 5A with the average structure represented by a ribbon in Figure 5B. The width of the ribbon in Figure 5B was modified to reflect the variance of the dihedral angle ϕ. The convergence of the calculated structures was analyzed using the angular order parameter S^{angle} (Hyberts et al., 1992), which ranges between the value zero for a completely random distribution of the particular torsion angle and the value 1 for an exactly defined torsion angle. The plots of S^{angle} for the dihedral angles ϕ, ψ, and χ_1, as well as the average dihedral angles ϕ and ψ, are presented in Figure 6B, C, D, and E.

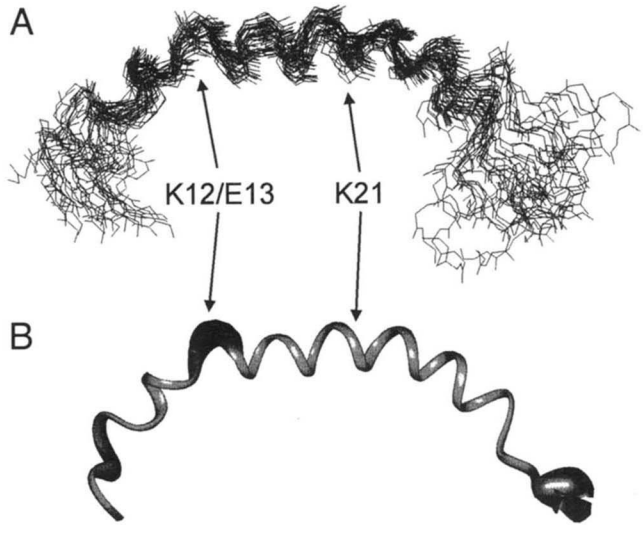

Fig. 5. A: The 28 calculated structures of apoC-I(1–38) with residues V4–K30 superimposed on the average structure. **B:** Ribbon representation of the average structure of apoC-I(1–38). The width of the ribbon was modified to reflect the circular variance of the dihedral angle ϕ.

Figure 5A and B shows that apoC-I(1–38) adopts a helical structure between residues V4 and K30 and an extended C-terminus from Q31 when bound to SDS. Analysis of the dihedral angles (Fig. 6E) and hydrogen bonds in the average structure with the DSSP program (Kabsch & Sander, 1983) indicates an α-helical conformation between residues L8 and L11, and F14 and K30, with residues V4–A7 forming a distorted helical turn. The conformational exchange in the region K12–G15, suggested by above-average H^N resonance linewidths, large temperature coefficients, and fast deuterium exchange, is reflected in the poor convergence of residues K12 and E13 (Fig. 5B) and the low order parameters of the K12/E13 dihedral angles (Fig. 6). Indeed, residues K12 and E13 divide the helix into two well-defined segments, V4–L11 and F14–K30, forming angles between 120 and 170°, with an average of 125°. The F14/G15 dihedral angles assume high order parameters (Fig. 6) because the observed NOEs were sufficient to restrain one of the two slowly exchanging conformations. The RMS deviations for the backbone trace (N, C^{α}, C′) of the 28 calculated structures to their average structure are 0.46 ± 0.21 Å for V4–L11, 0.59 ± 0.23 Å for F14–K30, but 1.24 ± 0.44 Å for V4–K30. Twelve hydrogen bonds between L8 and K30 were defined by C=O(i)···H-N(i + 3,4) distances of less than 2.5 Å and bond angles of 120–180° (Baker & Hubbard, 1984). The carbonyl groups of residues D9–K12 are not involved in hydrogen bonds, which may be attributed to the mobility of residues K12 and E13 and the concomitant bend in the long helical axis. Another disruption of the hydrogen bonding network within the region L8–K30 occurs at the carbonyl groups of E19 and D20, introducing a bend of 150° centered at K21. The two bends in apoC-I(1–38), defined by the nonhelical dihedral angles of K12/E13 and E19/D20 (Fig. 6E), produce an overall curvature of apoC-I(1–38) toward its hydrophobic face.

The orientation of the side chains in the region V4–K30 of apoC-I(1–38), illustrated in Figure 7, fits the general description of a class A_2 amphipathic helix (Segrest et al., 1990). The hydrophobic side chains are exclusively on the concave face, forming two

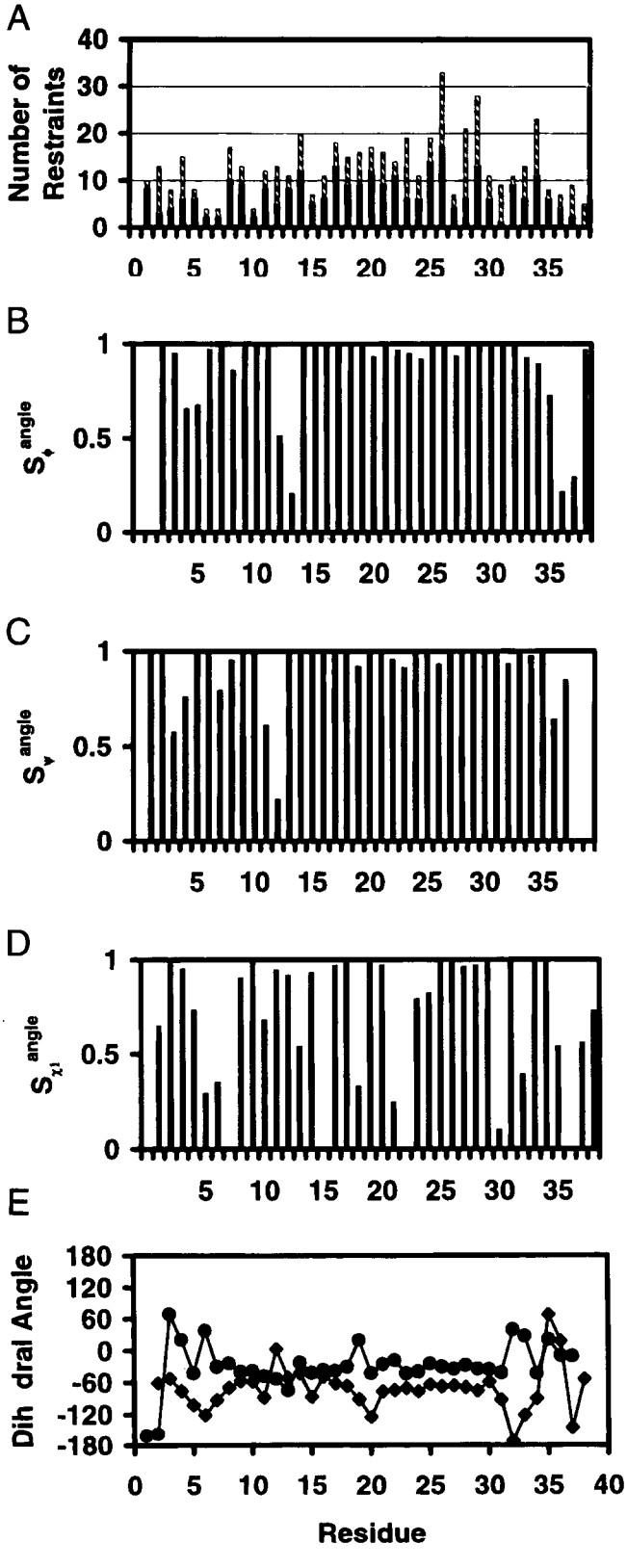

Fig. 6. A: Number and distribution of interresidue (filled columns) and intraresidue (hatched columns) NOE distance restraints used for structure calculation of apoC-I(1–38). **B,C,D:** Angular order parameters S^{angle} of the dihedral angles ϕ, ψ, and χ_1 calculated as described by Hyberts et al. (1992). **E:** Dihedral angles ϕ (diamonds) and ψ (circles) measured from the average of 28 calculated structures.

hydrophobic clusters, L8, L11, F14, and L18, and L25, I26, and I29. The positively charged side chains of lysines and arginines form three pairs, K10 and K12, K21 and R23, and R28 and K30, at the interface of the peptide. The negatively charged side chains are located on the hydrophilic face of the molecule with the exception of E19, which is at the interface.

Ion pair formation and side-chain pK_as

Several studies have suggested that intramolecular ion-pairing between oppositely charged side chains, separated by three or four residues, contributes to helix stability (Marqusee & Baldwin, 1987; Merutka & Stellwagen, 1991; Lyu et al., 1992). Examination of the helical region in the ensemble of structures calculated for apoC-I(1–38) shows that, of the six potential ion pairs, only one, E19 and R23, has an average O···N distance (4.7 ± 1.6 Å) which is near the O···N distance of 3.5 Å required for significant electrostatic interaction (Baker & Hubbard, 1984). In order to confirm the absence of ion pairs in apoC-I(1–38), the pK_as of some acidic amino acid side chains were determined by monitoring the pH-dependent change of chemical shifts of the methylene protons adjacent to the carboxyl groups. The pK_a values of side-chain carboxyl groups are 4.6 ± 0.1 for D3, 5.0 ± 0.1 for D9, 4.9 ± 0.1 for D20, and 6.8 ± 0.1 for E19. In proteins, the expected pK_a of aspartic or glutamic acid side chains not participating in ion pairs is 4.4–4.6 (Cantor & Shimmel, 1980); ion pair formation results in a lower pK_a (Pallaghy et al., 1995). The observed pK_a values of D3, D9, D20, and E19 are above or equal to 4.4–4.6, suggesting that these side chains are not involved in ion pairs. Note that the pK_a of E19 is shifted up by about two pH units compared to D3, D9, D20. Such an effect is likely due to the interfacial position of the E19 side chain (Fig. 7), where it is in close proximity to the micellar surface. The electrostatic effect of the negatively charged SDS head groups may cause a decrease in the local pH and an increase in the pK_a value of E19 (Spyracopoulos & O'Neil, 1994; Wang et al., 1996b). The 10% reduction in helical content of apoC-I(1–38) over the basic pH range, indicated by CD results, may be due to electrostatic repulsion between the deprotonated carboxyl group of residue E19 and the SDS head groups. The pK_a study and examination of distances between potential ion pair formers indicate that apoC-I(1–38) is not stabilized by intramolecular ion pairs. Similar conclusions were drawn for other amphipathic peptides (Rozek et al., 1995; Buchko et al., 1996; Dunne at al., 1996; Wang et al., 1996a, 1996b).

Discussion

Comparison of amphiphilic ligands

The helicity of apoC-I(1–38) bound to SDS and egg yolk lysoPC estimated from the CD data (55%) agrees well with the helical content determined by the DSSP analysis (Kabsch & Sander, 1983) of the NMR-derived average structure (55%). The similar helical content of apoC-I(1–38) when bound to SDS or egg yolk lysoPC, detergents with anionic or zwitterionic head groups, respectively, suggests that the amphipathic helix is stabilized primarily by the hydrophobic/hydrophilic interface provided by the detergent micelle (Buchko et al., 1996; Wang et al., 1996b). The content of helical secondary structure reported for apoC-I(1–38) when bound to egg yolk PC vesicles, 65% (Jackson et al., 1974), is slightly higher than in SDS or egg yolk lysoPC. The latter effect may be

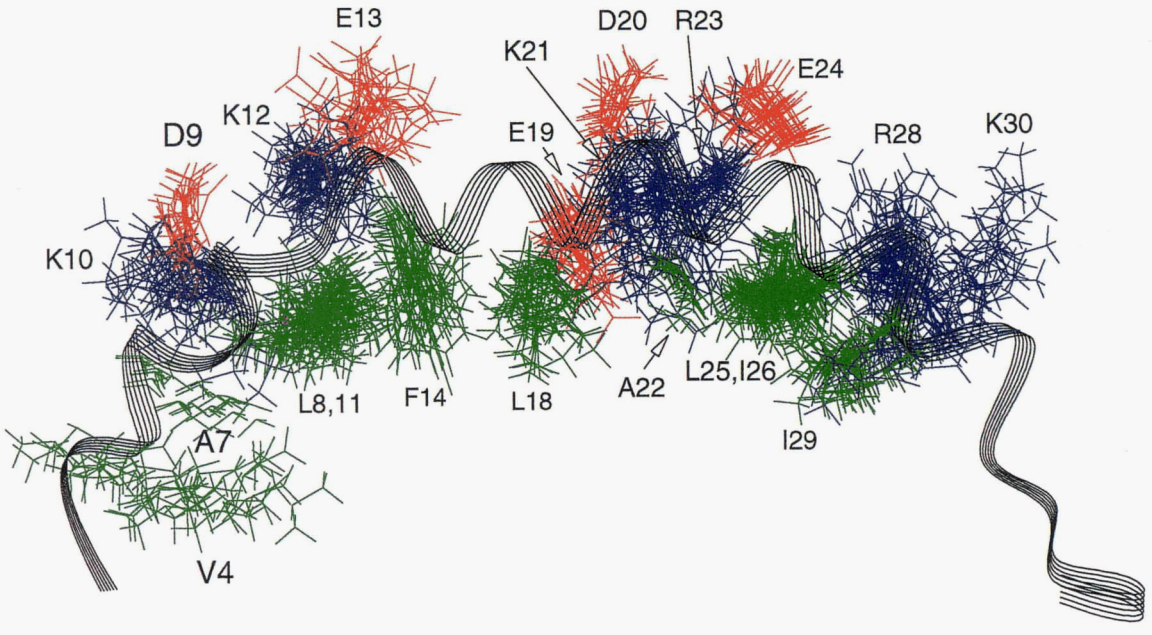

Fig. 7. Orientation of positively charged (blue), negatively charged (red), and nonpolar (green) side chains of residues V4–K30 of apoC-I(1–38). The backbone conformation of the average structure is included as a ribbon.

due to conversion of mobile regions, e.g., V4–A7 and K12–E13, into more regular helical structure in the larger complex with egg yolk PC, where maximum helicity is observed at a molar lipid to peptide ratio of 113 (Jackson et al., 1974) compared to 20 with SDS or egg yolk lysoPC.

Structural comparison of ApoC-I(1–38) with ApoC-I(7–24)

The residues involved in conformational exchange in apoC-I(1–38), K12–G15, are also contained in the shorter fragment apoC-I(7–24) whose structure was determined under similar experimental conditions and observed to adopt a continuous helix from D9 to K21 (Rozek et al., 1995). In Figure 8, the common helical regions of the average structures of both peptides, F14 to K21, are superimposed with RMS deviations of 0.42 Å (heavy backbone atoms) and 1.17 Å (all heavy atoms). The hydrophobic side chains of L11, F14, and L18 adopt very similar positions in both structures despite a different backbone geometry for L11. Due to the bend at K12 and E13 in apoC-I(1–38), the side chain of L8 is closer to the other hydrophobic residues than it would be in a straight helical conformation. The structural differences observed between apoC-I(7–24) and apoC-I(1–38) may arise for two reasons. First, in apoC-I(7–24), L8 is near the N-terminus, which shows some fraying in the calculated ensemble of structures and may not bind as tightly to SDS as the helical core of the peptide. On the other hand, in apoC-I(1–38), L8 likely associates strongly with SDS and forms a well-defined helical turn toward L11 as part of the hydrophobic cluster L8, L11, F14, and L18. Second, compared to apoC-I(7–24),

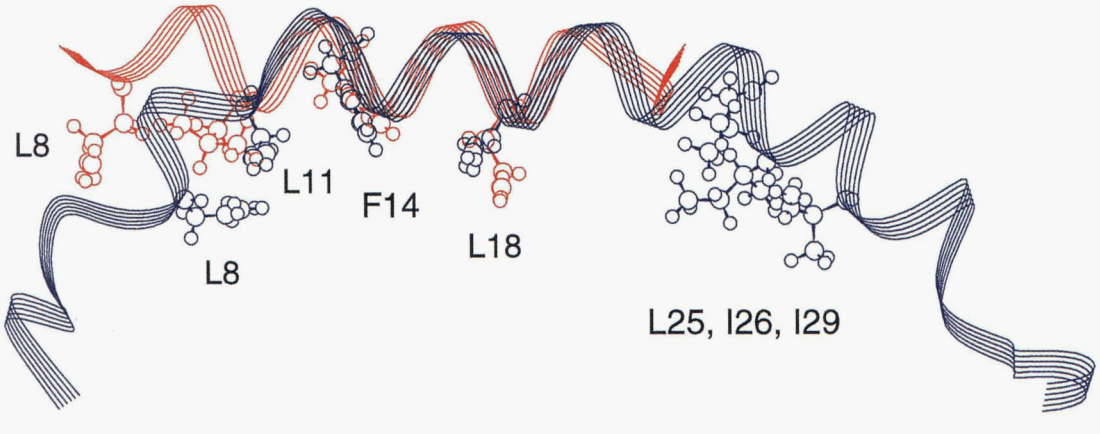

Fig. 8. Average structures of apoC-I(7–24) (red) and apoC-I(1–38) (blue) superimposed with residues 14–21. The side chains forming the hydrophobic clusters are shown. Note that side-chain geometry is distorted because the average structure represents mean atomic positions.

the hydrophobic face in apoC-I(1–38) is elongated by an additional hydrophobic cluster, L25, I26, and I29. The interaction between both hydrophobic binding sites and SDS likely leads to the curved conformation of the peptide where the apoC-I(1–38)–SDS complex is most stable. The lipid-associating apolipoprotein fragment apoE(263–286) was also observed to form a curved amphipathic helix–bend–helix structure in the presence of SDS (Wang et al., 1996a), which may be ascribed to the strong interaction of two hydrophobic binding sites, centered at W264/F265 and W276, with SDS.

Prediction of secondary structure and lipid-associating regions of apoC-I

The amino acid sequence of apoC-I(1–38) overlaps with the sequence of another previously studied peptide, apoC-I(35–53), which forms an amphipathic helix between residues 39 and 51 when bound to SDS (Rozek et al., 1995). Based on the structures of apoC-I(1–38) and apoC-I(35–53), we propose that apoC-I (57 residues) contains two lipid-associating amphipathic helical regions in the presence of SDS, spanning residues V4–K30 and R39–E51, with the N-terminal helix undergoing some conformational exchange about the region K12–G15. Analysis of the primary sequence of apoC-I by helical wheel algorithms suggests two amphipathic helices with a break centered at E33 (Segrest et al., 1992). Our data support such a helix break because the C-terminal eight residues of apoC-I(1–38) are unstructured, a feature that can be attributed to the loss of periodicity in the amino acid sequence required for the formation of an amphipathic helical structure.

We propose that the ability of apoC-I to associate with lipids is based mainly on hydrophobic clusters that are formed by the side chains of leucine and isoleucine and by the aromatic side chains of tryptophan and phenylalanine. Three such binding sites are formed by L8, L11, F14, and L18; L25, I26, and I29; and W41, F42, and F46. In previous studies, the apoC-I fragment 39–57 did not bind to PC, nor did it activate the enzyme LCAT, whereas the fragments 32–57, 24–57, and 17–57 bound to PC and activated LCAT 50%, 60%, and 100% relative to apoC-I, respectively (Sparrow et al., 1977). On the basis of our present structure determination, these results can be interpreted as the formation of (1) one lipid-binding site, W41, F42, and F46, in the fragments 32–57 and 24–57, which is unstable in the shorter fragment 39–57, and (2) two lipid-binding sites in the fragment 17–57, one at W41, F42, and F46, and the other at L25, I26, and I29.

ApoC-I is distributed between spherical HDL and VLDL particles, the diameters of which are estimated to be 4–10 nm and 25–70 nm, respectively (Scanu et al., 1982). The curvature in the calculated average conformation of apoC-I(1–38) is consistent with the size of a small HDL particle (4 nm). Furthermore, the flexible K12–G15 region may act as a hinge that allows the lipid-binding domain to adapt to both HDL and VLDL particle sizes.

Materials and methods

Synthesis of apoC-I(1–38)

ApoC-I(1–38), TPDVSSALDKLKEFGNTLEDKARELISRIKQSE LSAKM, was assembled on an ABI model 431A automated synthesizer using standard Fmoc-based solid-phase protocols supplied by the manufacturer. The AMPDA resin was synthesized as described by Kanda et al. (1991). The AMPDA resin hydrochloride salt (0.25 mmol, 0.35 g) was neutralized with 10% tetrabutylammonium hydroxide in methanol, washed with methanol, followed by dichloromethane, and dried under vacuum prior to loading with the carboxyl-terminal methionine. The sulfoxide derivative of the methionine was used to prevent alkylation by *tert*-butyl protecting groups released during final acidolytic deprotection and cleavage from the resin. The methionine sulfoxide was introduced onto the neutralized AMPDA resin as the 2,4,5-trichlorophenyl-3′-(4″-(*N*-α-Fmoc-methionine sulfoxide-oxymethyl)phenoxy)-propionate (*N*-α-Fmoc-methionine sulfoxide-TCP-HMPP), which was prepared essentially as described by Albericio and Barany (1985): *N*-α-Fmoc-methionine sulfoxide (2.60 mmol, 1.00 g) was mixed with 2,4,5-trichlorophenyl 3′-(4″-hydroxymethyl-phenoxy) propionate (TCP-HMPP) (1.50 mmol, 0.56 g) in 14 mL dichloromethane containing *N*,*N*-dimethylformamide dineopentyl acetal (2.60 mmol, 0.60 g). The product, *N*-α-Fmoc-methionine sulfoxide-TCP-HMPP, was crystallized from ethyl acetate-pentane at −20 °C (0.85 mmol, 0.63 g). The AMPDA resin (0.3 g) was resuspended in 4.0 mL of *N*-methylpyrrolidone containing 1-hydroxybenzotriazole (0.65 mmol, 0.10 g) and *N*-α-Fmoc-methionine sulfoxide-TCP-HMPP (0.54 mmol, 0.40 g). The mixture was shaken for two days at room temperature, filtered, and washed with *N*-methylpyrrolidone followed by dichloromethane. Ninhydrin analysis of the product, *N*-α-Fmoc methionine sulfoxide-HMPP resin, was negative; quantification of the reaction by piperidine release of the Fmoc group gave a loading of 0.42 mmol methionine/g resin. The N-α-Fmoc-methionine sulfoxide-HMPP resin (0.27 g, 0.11 mmol) and commonly protected amino acids were used to sequentially assemble apoC-I(1–38). The finished polypeptide was cleaved from the resin and fully deprotected with trifluoroacetic acid (TFA, 10 mL/g resin) in the presence of scavengers (phenol, 7.5% w/v; water, 5% v/v; and thioanisole, 5% v/v). The crude peptide was precipitated and washed (3×) with cold methyl *tert*-butyl ether, dissolved in 5% acetic acid, and desalted over a BioGel P-2 column. Fractions containing peptide were pooled and lyophilized. The recovery of crude peptide was about 70% of theoretical, based on 100% coupling efficiency. The carboxyl-terminal methionine sulfoxide was reduced to methionine with *N*-methylmercaptoacetamide as described by Houghten and Li (1979). Purification of apoC-I(1–38) was achieved by reverse-phase HPLC on a VyDac C-18 preparative column using a gradient of isopropanol, containing 0.08% (v/v) TFA, in aqueous (0.1%, v/v) TFA. The major HPLC band was repurified on a VyDac C18 semi-preparative column, then dialyzed extensively against water (5 × 2 L) and lyophilized to dryness. The composition of the major product, determined by amino acid analyses with a Beckman 7300 analyzer and System Gold software, corresponded to the sequence for apoC-I(1–38). The molecular weight of the product determined by electrospray ionization mass spectrometry (Finnegan MAT SSQ700 mass spectrometer) was within 0.3 mass units of the predicted molecular weight of 4,249.9 for apoC-I(1–38). The yield of reduced, purified apoC-I (1–38), based on the amount of crude peptide obtained from the resin, was about 20%.

CD spectroscopy

CD spectra of apoC-I(1–38) were obtained on a Jasco J710 spectropolarimeter calibrated using *d*-(+)-camphorsulfonate. ApoC-I(1–38) (0.05 mM at pH 6) was titrated with SDS (BDH Chemicals Ltd., Poole, England) or egg yolk lysoPC (Sigma, St. Louis, Missouri) at concentrations ranging from 0.0 to 4.0 mM. CD spectra of

apoC-I(1–38) (0.05 mM, 50 mM potassium chloride, 20 mM potassium phosphate, pH 5) in the presence of 0–70% (v/v) TFE (Sigma, St. Louis, Missouri) were also obtained. All measurements were performed in a quartz cell of 0.1 cm pathlength. The temperature was kept constant at varying values between 10 °C and 37 °C with a Neslab RTE-110 circulating water bath. Spectra were the average of two consecutive scans from 190 to 260 nm recorded with a bandwidth of 0.5 nm, a scan rate of 10 nm/min, and a time constant of 0.25 s. Following baseline correction, the observed ellipticities were converted to mean residue ellipticities, $[\Theta]$, in units of deg × cm^2/dmol. The helical content was estimated by deconvoluting the CD spectra using convex constraint analysis (Perczel et al., 1992) and from the $[\Theta]_{222}$ value using the relation % helix = $(|[\Theta]_{222}| + 3{,}000)/(36{,}000 + 3{,}000)$ (Greenfield & Fasman, 1969).

NMR spectroscopy

The NMR sample of apoC-I(1–38) (5 mM) was prepared by dissolving the lyophilized peptide in 500 μL of either 90% H_2O/10% D_2O or 99.9% D_2O (STOHLER/KOHR Stable Isotopes Inc., Cambridge, Massachusetts), containing 300 mM SDS-d_{25} (Cambridge Isotope Laboratories Inc., Andover, Massachusetts), or in an aqueous solution containing 50% (v/v) TFE-d_3 (Cambridge Isotope Laboratories Inc.)/10% D_2O, 50 mM potassium chloride, and 20 mM potassium phosphate (BDH Chemicals Ltd., Poole, England). The pH of all samples was adjusted to 4.8 ± 0.1 (uncorrected for the deuterium isotope effect).

NMR experiments were run on a Bruker AMX 600 spectrometer. TOCSY (Braunschweiler & Ernst, 1983; Bax & Davis, 1985), NOESY (Jeener et al., 1979), and DQF-COSY (Rance et al., 1983) spectra were recorded at 37 °C in the phase-sensitive mode using TPPI (Redfield & Kunz, 1975), collecting 512 t_1 increments and 32 transients in 2K data points. In TOCSY and NOESY experiments, the water was suppressed using the WATERGATE technique (Piotto et al., 1992), which employed the 3-9-19 pulse sequence (Sklenár et al., 1993). In the DQF-COSY experiment, obtained in 99.9% D_2O, the residual HDO signal was suppressed during the recycling delay (1.5 s). TOCSY spectra were acquired using the MLEV-17 spin-locking sequence at mixing times of 100, 120, and 160 ms. NOESY data were recorded with mixing times of 50, 75, 100, 150, and 200 ms.

Spectra were processed with UXNMR on an Aspect workstation (Bruker). Prior to Fourier transformation, the data were zero-filled to generate a 2K × 1K matrix. Resolution enhancement was accomplished by apodization with a 0° shifted quadratic sine-bell window function in F1 and a 90° shifted quadratic sine-bell function in F2. Baseline corrections with a fifth-order polynomial function were applied in both dimensions. Chemical shifts were referenced to external DSS.

Temperature coefficients for the amide resonances of apoC-I(1–38) in SDS-d_{25} were obtained by recording NOESY spectra between 25 °C and 50 °C in steps of 5 degrees. The amide chemical shift was plotted as a function of temperature and the plot analyzed by linear regression to extract the slope.

The deuterium exchange experiments were performed by lyophilizing the 90% H_2O/10% D_2O NMR sample of apoC-I(1–38) in SDS at pH = 4.8 ± 0.1 and adding 99.9% D_2O. To assign slowly exchanging amide protons, a NOESY spectrum was recorded at 37 °C 2 h after adding D_2O.

The pK_a values of the D3, D9, E19, and D20 side-chain carboxyl groups were determined by monitoring the pH-dependent chemical shifts of the β- and γ-protons of aspartic and glutamic acid, respectively, by 2D NMR, and fitting the data to a modified Henderson–Hasselbach equation. The pH values were not corrected for the deuterium isotope effect.

NOE classification and structure calculation

The NOE cross-peak volumes of the NOESY spectrum at 150 ms mixing time were grouped into three overlapping distance classes, 1.8–3.0 Å, 2.5–4.0 Å, and 3.5–5.0 Å, to reflect the uncertainty in NOE intensity due to different internal molecular motions and spectral overlap. The upper and lower distance bounds were adjusted for pseudoatoms and nonstereospecifically assigned methylene protons and methyl groups using the NMR-Refine module of Insight II 95.0 (Biosym/MSI, San Diego, California). An additional correction of 0.5 Å was added to the upper bounds of methyl groups. Structure calculations were performed with the DGII program of Insight II 95.0 as described in Rozek et al. (1995).

Acknowledgments

We are grateful to Dr. Susan Weintraub of the University of Texas Health Sciences Center in San Antonio for kindly performing the mass spectral analysis of the apoC-I(1–38) peptide. We also thank Guangshun Wang and Rasmus Storjohann for fruitful discussions. This work was supported by the Heart and Stroke Foundation of B.C. & Yukon, and the Natural Science and Engineering Research Council of Canada (grants 669006 and OGP0009709, respectively). A.R. and G.W.B. are recipients of fellowships of the Heart and Stroke Foundation of B.C. & Yukon.

References

Albericio F, Barany G. 1985. Improved approach for anchoring N^{α}-9-fluorenylmethyloxycarbonylamino acids as *p*-alkoxybenzyl esters in solid-phase peptide synthesis. *Int J Peptide Protein Res 26*:92–97.

Bai Y, Milne JS, Mayne L, Englander SW. 1993. Primary structure effects on peptide group hydrogen exchange. *Proteins Struct Funct Genet 17*:75–86.

Baker EN, Hubbard RE. 1984. Hydrogen bonding in globular proteins. *Prog Biophys Mol 44*:97–179.

Bax A, Davis DG. 1985. MLEV-17-based two-dimensional homonuclear magnetization transfer spectroscopy. *J Magn Reson 65*:355–360.

Braunschweiler L, Ernst RR. 1983. Coherence transfer by isotropic mixing: Application to proton correlation spectroscopy. *J Magn Reson 53*:521–528.

Buchko GW, Wang G, Pierens GK, Cushley RJ. 1996. Conformational studies of an amphipathic peptide corresponding to human apolipoprotein A-II residues 18–30 with a C-terminal lipid binding motif, EWLNS. *Int J Peptide Protein Res 48*:21–30.

Cantor CR, Shimmel PR. 1980. *Biophysical chemistry. Part I: The conformation of biological macromolecules*. San Francisco, California: W.H. Freeman and Company.

Clifton-Bligh P, Nestel PJ, Whyte HM. 1972. Tangier disease. Report of a case and studies of lipid metabolism. *New Engl J Med 286*:567–571.

Dunne SJ, Cornell RB, Johnson JE, Glover NR, Tracey AS. 1996. Structure of the membrane binding domain of CTP:phosphocholine cytidyltransferase. *Biochemistry 35*:11975–11984.

Englander SW, Wand AJ. 1987. Main-chain-directed strategy for the assignment of ^{1}H NMR spectra of proteins. *Biochemistry 26*:5953–5958.

Glomset JA. 1968. The plasma lecithin:cholesterol acyltransferase reaction. *J Lipid Res 9*:155–167.

Greenfield N, Fasman GD. 1969. Computed circular dichroism spectra for the evaluation of protein conformation. *Biochemistry 8*:4108–4116.

Henry GD, Sykes BD. 1994. Methods to study membrane protein structures in solution. *Methods Enzymol 239*:515–535.

Holzwarth GM, Doty P. 1965. The ultraviolet circular dichroism of polypeptides. *J Am Chem Soc 87*:218–228.

Houghten RA, Li CH. 1979. Reduction of sulfoxides in peptides and proteins. *Anal Biochem 98*:36–46.

Hyberts SG, Goldberg MS, Havel TF, Wagner G. 1992. The solution structure of eglin c based on measurements of many NOEs and coupling constants and its comparison with X-ray structures. *Protein Sci 1*:736–751.

Jackson RL, Morrisett JD, Sparrow JT, Segrest JP, Pownall HJ, Smith LC, Hoff HF, Gotto AM Jr. 1974. The interaction of apolipoprotein-serine with phosphatidylcholine. *J Biol Chem 249*:5314–5320.

Jeener J, Meier BH, Bachmann P, Ernst RR. 1979. Investigation of exchange processes by two-dimensional NMR spectroscopy. *J Chem Phys 71*:4546–4553.

Jonas A. 1986. Synthetic substrates of lecithin:cholesterol acyltransferase. *J Lipid Res 27*:689–698.

Kabsch W, Sander C. 1983. Dictionary of protein secondary structure: Pattern recognition of hydrogen-bonded and geometrical features. *Biopolymers 22*:2577–2637.

Kanda P, Dunham RG, Hasan SQ, Weintraub ST, Kushwaha RS. 1994. Synthetic apolipoprotein C-I peptide inhibition of cholesteryl ester transfer protein activity in baboon plasma. In: Hodges RS, Smith JA, eds. *Peptides: Chemistry, structure and biology. Proceedings of the Thirteenth American Peptide Symposium*. ESCOM, Leiden. pp 408–409.

Kanda P, Kennedy RC, Sparrow JT. 1991. Synthesis of polyamide supports for use in peptide synthesis and as peptide-resin conjugates for antibody production. *Int J Peptide Protein Res 38*:385–391.

Koizumi J, Inazu A, Yagi K, Koizumi I, Uno Y, Kajinami K, Miyamato S, Molin P, Tall AR, Mabuchi H. 1991. Serum lipoprotein lipid concentration and composition in homozygous and heterozygous patients with cholesteryl ester transfer protein deficiency. *Atherosclerosis 90*:189–196.

Koizumi J, Mabuchi H, Yoshimura A, Michishita I, Takeda M, Itoh H, Sakai Y, Sakai T, Ueda K, Takeda R. 1985. Deficiency of serum cholesteryl-ester transfer activity in patients with familial hyperalphalipoproteinaemia. *Atherosclerosis 58*:175–186.

Kushwaha RS, Hasan SQ, McGill HCJ, Getz GS, Dunham RG, Kanda P. 1993. Characterization of cholesteryl ester transfer protein inhibitor from plasma of baboons (*Papio* sp.). *J Lipid Res 34*:1285–1297.

Lyu PC, Gans PJ, Kallenbach NR. 1992. Energetic contribution of solvent-exposed ion pairs to alpha-helix structure. *J Mol Biol 223*:343–350.

Marqusee S, Baldwin RL. 1987. Helix stabilization by $glu^- \cdots lys^+$ salt bridges in short peptides of de novo design. *Proc Natl Acad Sci USA 84*:8898–8902.

McDonnell PA, Opella SJ. 1993. Effect of detergent concentration on multidimensional solution NMR spectra of membrane proteins in micelles. *J Magn Res B 102*:120–125.

Merutka G, Stellwagen E. 1991. Effect of amino acid ion pairs on peptide helicity. *Biochemistry 30*:1591–1594.

Miller GJ, Miller NE. 1975. Plasma-high-density-lipoprotein concentration and development of ischæmic heart-disease. *Lancet 1*:16–19.

Morton RE, Greene DJ. 1994. Enhanced detection of lipid transfer inhibitor protein activity by an assay involving only low density lipoprotein. *J Lipid Res 35*:2094–2099.

Morton RE, Steinbrunner JV. 1993. Determination of lipid transfer inhibitor protein activity in human lipoprotein-deficient plasma. *Atherosclerosis and Thrombosis 13*:1843–1851.

Morton RE, Zilversmit DB. 1982. Purification and characterization of lipid transfer protein(s) from human lipoprotein-deficient plasma. *J Lipid Res 23*:1058–1067.

Nishide T, Tollefson JH, Albers JJ. 1989. Inhibition of lipid transfer by a unique high density lipoprotein subclass containing an inhibitor protein. *J Lipid Res 30*:149–158.

Pallaghy RK, Scanlon MJ, Monks SA, Norton RS. 1995. Three-dimensional structure in solution of the polypeptide cardiac stimulant anthopleurin-A. *Biochemistry 34*:3782–3794.

Perczel A, Park K, Fasman GD. 1992. Analysis of the circular dichroism spectrum of proteins using the convex constraint algorithm: A practical guide. *Anal Biochem 203*:83–93.

Piotto M, Saudek V, Sklenár V. 1992. Gradient-tailored excitation for single-quantum NMR spectroscopy of aqueous solutions. *J Biomol NMR 2*:661–665.

Rance M, Sørensen OW, Bodenhausen G, Wagner G, Ernst RR, Wüthrich K. 1983. Improved spectral resolution in COSY ^{1}H NMR spectra of proteins via double quantum filtering. *Biochem Biophys Res Commun 117*:479–485.

Redfield AG, Kunz SD. 1975. Quadrature Fourier NMR detection: Simple multiplex for dual detection and discussion. *J Magn Reson 19*:250–254.

Rohl CA, Baldwin RL. 1994. Exchange kinetics of individual amide protons in ^{15}N-labeled helical peptides measured by isotope-edited NMR. *Biochemistry 33*:7760–7767.

Rozek A, Buchko GW, Cushley RJ. 1995. Conformation of two peptides corresponding to human apolipoprotein C-I residues 7–24 and 35–53 in the presence of sodium dodecyl sulfate by CD and NMR spectroscopy. *Biochemistry 34*:7401–7408.

Scanu AM, Edelstein C, Shen BW. 1982. Lipid–protein interactions in plasma lipoproteins. Model: High density lipoprotein. In: Jost PC, Griffith OH, eds. *Lipid–protein interactions*. New York: John Wiley & Sons. pp 259–316.

Schaefer EJ, Ordovas JM, Law SW, Ghiselli G, Kashyap, Srivastava LS, Heaton WH, Albers JJ, Connor WE, Lindgren FT, Lemeshev Y, Segrest JP, Brewer HB Jr. 1985. Familial apolipoprotein A-I and C-III deficiency, variant II. *J Lipid Res 26*:1089–1099.

Segrest JP, De Loof H, Dohlman JG, Brouillette CG, Anantharamaiah GM. 1990. The amphipathic helix motif: Classes and properties. *Proteins Struct Funct Genet 8*:103–117.

Segrest JP, Jackson RL, Morrisett JD, Gotto AM Jr. 1974. A molecular theory of lipid–protein interactions in the plasma lipoproteins. *FEBS Lett 38*:247–253.

Segrest JP, Jones MK, De Loof H, Brouillette CG, Venkatachalapathi YV, Anantharamaiah GM. 1992. The amphipathic helix in the exchangeable apolipoproteins: A review of secondary structure and function. *J Lipid Res 33*:141–166.

Sehayek E, Eisenberg S. 1991. Mechanisms of inhibition by apolipoprotein C of apolipoprotein E-dependent cellular metabolism of human triglyceride-rich lipoproteins through the low density lipoprotein receptor pathway. *J Biol Chem 266*:18259–18267.

Sklenár V, Piotto M, Leppik R, Saudek V. 1993. Gradient-tailored water suppression for ^{1}H-^{15}N HSQC experiments optimized to retain full sensitivity. *J Magn Reson A 102*:241–245.

Son YS, Zilversmit DB. 1984. Purification and characterization of human plasma proteins that inhibit lipid transfer activities. *Biochim Biophys Acta 795*:473–480.

Soutar AK, Garner CW, Baker HN, Sparrow JT, Jackson RL, Gotto AM, Smith LC. 1975. Effect of the human plasma apolipoproteins and phosphatidylcholine acyl donor on the activity of lecithin:cholesterol acyltransferase. *Biochemistry 14*:3057–3064.

Sparrow JT, Pownall HJ, Sigler GF, Smith LC, Soutar AK, Gotto AM Jr. 1977. The mechanism of phospholipid binding by the plasma apolipoproteins. In: Goodman M, Meienhofer J, eds. *Peptides: Proceedings of the Fifth American Peptide Symposium*. New York: John Wiley & Sons. pp 149–152.

Spyracopoulos L, O'Neil JDJ. 1994. Effect of a hydrophobic environment on the hydrogen exchange kinetics of model amides determined by ^{1}H-NMR spectroscopy. *J Am Chem Soc 116*:1395–1402.

Steyrer E, Kostner GM. 1988. Activation of lecithin:cholesterol acyltransferase by apolipoprotein D: Comparison of proteoliposomes containing apolipoprotein D, A-I or C-I. *Biochim Biophys Acta 958*:484–491.

Swaney JB, Weisgraber KH. 1994. Effect of apolipoprotein C-I peptides on the apolipoprotein E content and receptor-binding properties of beta-migrating very low density lipoproteins. *J Lipid Res 35*:134–142.

Tall AR. 1993. Plasma cholesteryl transfer protein. *J Lipid Res 34*:1255–1274.

Wagner G, Wüthrich K. 1982. Amide proton exchange and surface conformation of the basic pancreatic trypsin inhibitor in solution. *J Mol Biol 160*:343–361.

Wang G, Pierens GK, Treleaven WD, Sparrow JT, Cushley RJ. 1996a. Conformations of human apolipoprotein E(263–286) and E(267–289) in aqueous solutions of sodium dodecyl sulfate by CD and ^{1}H NMR. *Biochemistry 35*:10358–10366.

Wang G, Treleaven WD, Cushley RJ. 1996b. Conformation of human serum apolipoprotein A-I(166–185) in the presence of sodium dodecyl sulfate or dodecylphosphocholine by ^{1}H-NMR and CD. Evidence for specific peptide-SDS interactions. *Biochim Biophys Acta 1301*:174–184.

Weisgraber KH, Mahley RW, Kowal RC, Herz J, Goldstein JL, Brown MS. 1990. Apolipoprotein C-I modulates the interaction of apolipoprotein E with β-migrating very low density lipoproteins (β-VLDL) and inhibits binding of β-VLDL to low density lipoprotein receptor-related protein. *J Biol Chem 265*:22453–22459.

Wishart DS, Bigam CG, Holm A, Hodges RS, Sykes BD. 1995. ^{1}H, ^{13}C and ^{15}N random coil NMR chemical shifts of the common amino acids. I. Investigation of nearest-neighbor effects. *J Biomol NMR 5*:67–81.

Wishart DS, Sykes BD, Richards FM. 1991. Relationship between nuclear magnetic resonance chemical shift and protein secondary structure. *J Mol Biol 222*:311–333.

Wishart DS, Sykes BD, Richards FM. 1992. The chemical shift index: A fast and simple method for the assignment of protein secondary structure through NMR spectroscopy. *Biochemistry 31*:1647–1651.

Woody RW. 1977. Optical rotary properties of biopolymers. *J Polymer Sci Macromol Rev 12*:181–320.

Wüthrich K. 1986. *NMR of proteins and nucleic acids*. New York: John Wiley & Sons.

Yokoyama S, Kurasawa T, Nishikawa O, Yamamoto A. 1986. High density lipoproteins with poor reactivity to cholesterol ester transfer reaction observed in a homozygote of familial hyperalphalipoproteinemia. *Artery 14*:43–51.